3-2020

Integration Concept of Injection, Forming and Foaming: A Practical Approach to Manufacture Hybrid Structures

Saeed Farahani

Sai Aditya Pradeep

Srikanth Pilla

Integration Concept of Injection, Forming and Foaming: A Practical Approach to Manufacture Hybrid Structures

Saeed Farahani[1,2], Sai Aditya Pradeep[1,2] and Srikanth Pilla[1,2,3,4*]

[1] Department of Automotive Engineering, Clemson University, Greenville, SC, 29607, USA
[2] Clemson Composites Center, Clemson University, Greenville, SC, 29607, USA
[3] Department of Material Science and Engineering, Clemson University, SC 29634, USA
[4] Department of Mechanical Engineering, Clemson University, Clemson, SC, 29634, USA
* Corresponding author
sfaraha@clemson.edu (Saeed Farahani), spradee@clemson.edu (Sai Aditya Pradeep) spilla@clemson.edu (Srikanth Pilla)

Abstract. Motivated by the concept of the integrative production systems, the hybrid process of polymer injection molding and sheet metal forming, known as polymer injection forming (PIF), has been introduced to manufacture sheet metal-polymer components in a single operation. Despite the wide potential application of this technology, its implementation in actual industrial production has been hindered due to several challenges; a thick layer of polymer where there is deep deformation, non-uniform deformation due to pressure loss and the opposite phenomena of shrinkage and springback. To mitigate these practical issues, the novel idea of integrating supercritical fluid (Sc.F.) technology with the PIF process is introduced in this work. As the proposed technology is a manufacturing innovation, with no available information in the literature correlating to this concept, two sets of experiments are designed to investigate the feasibility of this integration. In the first set, the effect of blank material and shot volume as design variables were investigated over a range of Sc.F. weight percentage. To improve the cell morphology in experiments with the low-strength sheet material, several other processing scenarios are explored in the second set of experiments. The results of this study clearly demonstrate the capabilities of this concept manufacturing process in terms of initiating the foaming process within the simultaneous injection/forming process, ensuring weight reduction (of up to 16 %) and complete elimination of issues related to shrinkage.

Keywords: polymer injection forming (PIF), supercritical fluid (Sc.F.) technology, hybrid structures

1 Introduction

1.1 Polymer Injection Forming (PIF)

Hybrid production system (HPS) involves the combination of multiple, diverse material systems (i.e. plastics and metals), which is of great interest for the complementary

characteristics they offer to a single hybrid component [1]. Although several processes are used to produce metal-polymer hybrid components, all of them involve issues such as a large number of processing steps and limitations in terms of both productivity and complexity for the component produced [2]. Motivated by the aforementioned aspects, a new platform technology has been recently developed to manufacture sheet metal-polymer macro composites in a single operation – known as Polymer Injection Forming (PIF) [3]. PIF is a hybrid production system that integrates the best-in-class manufacturing technologies in polymers and metals, viz., injection-molding and sheet metal forming. However, injection molding and sheet metal forming have differing physical principles (materials and process levels) and working mechanisms. Hence, while combining these methods can lead to increased output – which meets the objectives of using HPS – it is also a challenging initiative [4]. A schematic of the PIF process is shown in **Error! Reference source not found.**.

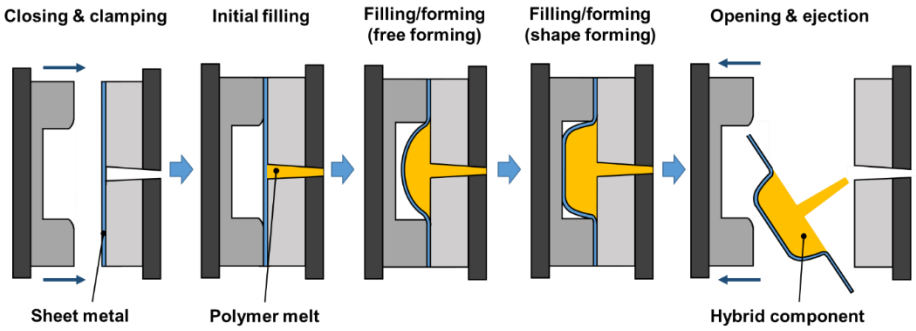

Fig. 1. Schematic of the PIF Process

During this process, the sheet metal blank is first placed into the mold cavity, followed by the injection of polymer melt. This melt serves as a pressure medium to deform/shape the blank during the filling stage of the injection molding process. After the injection stage, the polymer-metal joint is also achieved after solidification of the system by either thermal bonding, mechanical interlock or adhesive coating [5]. The solidified polymer remains as a reinforcing or functional element, depending upon the targeted design. PIF improves the production process/cycle by reducing the number of production steps while facilitating easy assembly via embedding several functionality features into a single product. Only a single tool is needed in PIF, thus greatly reducing tool costs [6].

1.2 Supercritical Fluid (Sc.F.) assisted injection molding

Supercritical fluid (Sc.F.) assisted injection molding is a unique technology in which CO_2 or N_2 in a supercritical state is used to form structural foamed products with superior strength-to-weight and cost-to-performance ratios to that of conventional injection-molded products [7]. In this process, after solid polymer reaches its molten state at the midpoint of the injection molding barrel, Sc.F. is introduced into the barrel via an

auxiliary metering system. Both Sc.F. and the polymer melt continue through the barrel, undergoing shear mixing in which the polymer melt is super-saturated with the Sc.F. fluid. This high-pressure single-phase solution is then injected into the mold cavity at atmospheric pressure (below the gas saturation pressure). This pressure drop below the saturation point triggers thermodynamic instability, inducing cell nucleation. Cell growth is controlled by gas diffusion rate and the stiffness of polymer-gas solution which directly influence the morphology of the part after solidification [8]. The benefits of Sc.F. assisted injection molding (SFAIM) technology are listed in **Error! Reference source not found.** along with a brief reasoning for each benefit [9].

Table 1. A list of benefits achievable by implementing Sc.F. assisted injection molding technology

Benefits	Reasoning
Part weight reduction	Due to creating the foamed core of the injected part
Faster cycles	Due to the elimination of packing phase and reduction in cooling time
Lower injection pressure	Due to lower viscosity of polymer melts with dissolved Sc.F.
Lower clamping force	Due to lower injection pressure
Reduced energy consumption	Due to the reduction in required injection pressure, clamping force and cooling time
Less shrinkage	Polymer melts with dissolved Sc.F. tends to expand rather than shrink.
Less warpage and sink marks	Due to the less shrinkage and more uniform cooling condition

1.3 Supercritical Fluid-assisted Polymer Injection Forming (SFPIF)

PIF is an HPS with the potential for expanding manufacturing research through the creation of multi-material constructs. However, several practical issues hinder its use in industrial applications. Comparing these hindrances with the benefits of Sc.F. technology (**Error! Reference source not found.**) shows the synergy of integrating these two processes. For example:

- A thick polymeric part resides (after solidification) at the location where the sheet is considered to deform deeply by means of melt pressure. This thick layer of polymer is not desired in conventional injection molding process for multiple reasons: (i) it increases the weight of the part; and (ii) It causes several issues such as increasing cooling time, possibility of warpage and local excessive shrinkage or sink marks.

Such issues were observed in some of our initial experiments as shown in **Error! Reference source not found.**(a). Therefore, integration of PIF with Sc.F. technology can maintain the lightweight condition owing to the nature of foaming process and eliminate the issues such as warpage and sink marks due to the significantly lesser shrinkage in the SFAIM process.

- The flow of polymer melt through a thin channel increases pressure loss along the flow path due to the viscous nature of melt. This excessive pressure loss causes a non-uniform pressure distribution and consequently non-uniform deformation as reported in prior works [10] and schematically illustrated in **Error! Reference source not found.**(b). Therefore, combining PIF with Sc.F. injection molding can help overcome this drawback as the dissolution of Sc.F. into the polymer melt significantly reduces its viscosity and thereby ensures uniformity in sheet metal deformation.
- Shrinkage and springback are common problems in injection molding and sheet metal forming, both of which play opposite roles in the hybrid PIF process, inducing significant residual stresses on the contact area that in turn reduces the bonding strength and leads to the delamination of sheet metal from the polymeric part (see **Error! Reference source not found.**(c)). Although reverse geometrical modification can compensate springback in conventional sheet metal forming processes, it is an imperfect solution for the PIF process as the injected polymer takes the deformed sheet shape and shrinks from that point. Therefore, reducing the residual stress and geometrical instability is possible by integrating PIF with Sc.F. injection molding as the polymer melt with dissolved Sc.F. tends to expand more (and shrink less), and such less shrinkage is one of the main benefits of Sc.F. assisted technology.

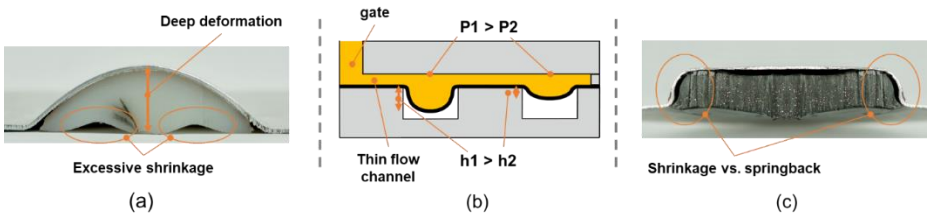

Fig. 2. Major practical issues associated with the application of the PIF process (Figure 2(b) was reproduced from [10])

Given the aforementioned benefits of conducting PIF process with Sc.F. technology, SFPIF – the integration of both processes – will yield lightweight, hybrid polymer-metal components for use in automotive, aerospace, and home appliance applications. As the proposed technology is a transformative manufacturing innovation, with nothing in literature relating to this concept, two sets of experiments based on different processing scenarios are designed to investigate the feasibility of this integration.

2 Design of experiments and process settings

In the first set of experiments, it was assumed that the optimum process parameters of the SFPIF process is identical to that of the regular SFAIM process. Hence, all the parameters except the Sc.F. dosing time and shot volume were set based on the optimum condition previously obtained in our experiments related to regular SFAIM process as listed in **Error! Reference source not found.**. Unless otherwise mentioned, all parameters listed in this table remain identical for all the experiments.

Table 2. A summary of fixed process parameters in this study

Clamp force	Inj. rate	Melt temp.	Mold temp.	switch over	Cool. time	Back press.	Sc.F. press.	Sc.F. Rate
100 kN	30 cm3/s	240 °C	35 °C	99% volume	120 s	150 bar	200 bar	0.07 kg/h

The weight percentage of the Sc.F. (defined by dosing time) was considered as one of the plasticizing parameters in order to examine its influence on the deformation of the sheet metal and the morphology of the final foamed part. Regarding the molding parameters, the shot volume was chosen as another variable parameter given its direct effect on the depth of deformation and consequently the thickness of the polymeric region. Two aluminum alloys (AA1100 and AA6061) exhibiting a significant difference in the strength and formability were considered for the sheet metal blank to investigate the expected effect of the sheet strength on the melt pressure and consequently on the cell morphology of the foamed part. The polymer selected as the injected material is ADX-2075 from Advanced Composites, Inc. It is an impact-resistant thermoplastic composed of polypropylene, rubber, and talc as fillers. The high melt flow rate (MFR) of 29 g/10 min and the fillers make this polymer a suitable option for the Sc.F. foaming process. Given all, the first set of the experiments were designed as listed in **Error! Reference source not found.**.

Table 3. Variable parameters in the first design of experiments (E1)

Effect of the Sc.F. dosing time					
Blank: AA1100				**Blank: AA6061**	
Shot volume: 30 cm^3		**Shot volume: 20 cm^3**		**Shot volume: 20 cm^3**	
Exp. #	**Dosing time (s)**	**Exp. #**	**Dosing time (s)**	**Exp. #**	**Dosing time (s)**
E1-1	0	E1-5	0	E1-8	0
E1-2	2	E1-6	4	E1-9	4
E1-3	4	E1-7	6	E1-10	6
E1-4	6				
Effect of shot volume at constant dosing time of 4 s					

Blank: AA1100		Blank: AA6061	
Exp. #	**Shot volume (cm^3)**	**Exp. #**	**Shot volume (cm^3)**
E1-11	**20**	E1-14	20
E1-12	**26**	E1-15	26
E1-13	**30**	E1-16	30

The results of the first set, as will be later shown and discussed in Section 4.4 (Figure 8), revealed that a microcellular morphology cannot be achieved by only variation of Sc.F. percentage, especially in the experiments with low strength sheet materials (AA1100). Hence, in the second set of the experiments, several other processing scenarios were examined to see whether it is possible to improve the cell morphology in low cavity pressure condition. In this regard, influence of injection speed, eliminating packing phase and adding decompression action (before plasticizing phase) were examined in the second set of experiments as listed in **Error! Reference source not found.**.

Table 4. Variable parameters in the second design of experiments (E2)

Blank: AA1100			
Shot volume: 20 cm^3			
Injection rate: 30 cm3/s		**Injection rate: 300 cm3/s**	
Exp. #	**Variable parameters**	**Exp. #**	**Variable parameters**
E2-1	5 s packing	E2-4	5 s packing
E2-2	No packing	E2-5	No packing
E2-3	No pack + decompress.	E2-6	No pack + decompress.

3 Measurements and sample preparation

Both the sheet metal blank (before the experiment) and final hybrid part (after completion of each experiment) were weighed to record the weight of the injected part. Then, the height and volume of the deformation were determined by measuring the deform sheet metal. To assess the light-weighting potential of the proposed SCPIF process, the density of the injected parts was calculated and compared with the density of the injected parts with zero percent Sc.F. (regular PIF). Using these values, the light-weighting percentage of each experiment was calculated using Equation **Error! Reference source not found.** where ρ_0 is the density of the solid part and ρ is the density of the foam part.

$$Lightweighting = \left(\frac{\rho_0 - \rho}{\rho_0}\right) * 10 \qquad (1)$$

The supercritically foamed samples were imaged at the cross-section using the following procedure, as demonstrated in **Error! Reference source not found.**:

1. A blade is used to notch the flat face of the samples along their diameters.
2. The samples are immersed in a dewar of liquid nitrogen for 45 minutes.
3. The samples are removed, secured in a vise and cryogenically fractured via rubber mallet.
4. Double-sided carbon tape is used to secure the fractured samples on an SEM sample mount.
5. The samples are inside a Hummer 6.2 sputtering system for 3 mins to deposit a thin layer of platinum on the non-conducting polymeric part of the hybrid samples.
6. The sputter-coated samples are imaged in a Hitachi 3400S scanning electron microscope at a maximum working distance to maximize the field of view. They are then subjected to an accelerating voltage of 5 kV at different magnifications to characterize cell size and density.

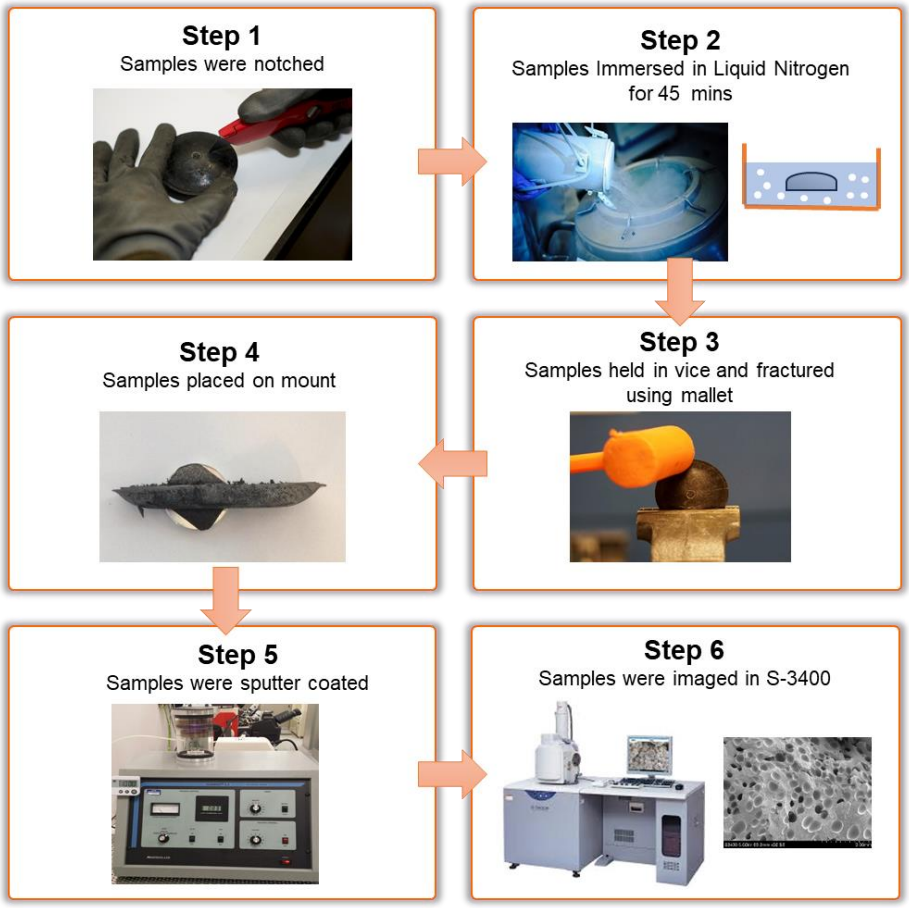

Fig. 3. Procedure followed to study foam morphology

The imaged samples were processed using Image J analysis tool to calculate the average cell size and cell density. Cell density, in particular, was calculated using Equation **Error! Reference source not found.**, where N is the number of cells, L is the linear length of the area, and M is a unit conversion, resulting in cell density being expressed as the number of cells per cubic centimeter [11]. In order to avoid skewing of data, a few abnormally large voids observed in some specimens were excluded from the calculation of average cell size and cell density.

$$Cell\ density\ = \left(\frac{N}{L^2}\right)^{\frac{3}{2}} M \qquad (2)$$

As the main objective of this work is to explore the feasibility of this integration (the SFPIF process) and its capabilities in eliminating the PIF issues, the replication of the experiments has been limited to the plasticizing stage in order to make sure about processing a uniform solution of polymer melt and Sc.F. before injection stage. But the rest of the experimental procedure and measurements have been restricted to a single experiment with no replications.

4 Results and feasibility of integration concept

4.1 Initial trials and observation

It was determined during the initial trials that a proper adjustment of the process parameters related to the plasticizing stage is deemed most necessary in terms of achieving a uniform single-phase solution of Sc.F. and polymer melt. Otherwise, the injection of the polymer melt and Sc.F. as two separated phases would result in large empty spaces within the polymeric region, which is detected only by cutting the samples as shown in **Error! Reference source not found.**(a). The other defect observed especially on the sample with a thick layer of polymer (experiments with shot volume 30 cm^3) was a bump on the side of the part that is not in contact with the sheet metal as shown in **Error! Reference source not found.**(b). This defect is attributed to insufficient cooling time as the unsolidified melt at the core of the sample expands after the ejection with a manifestation of the bulge on the outer surface of the sample.

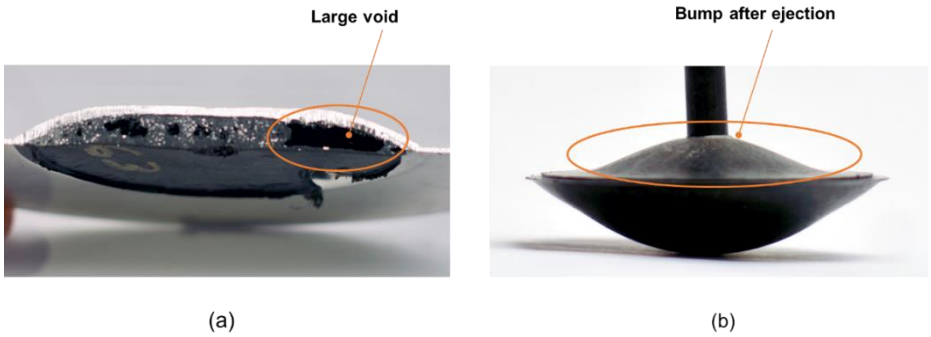

Fig. 4. Defects observed during initial trials

4.2 Dimensional properties and shrinkage

The height and volume of the deformation shown in **Error! Reference source not found.** is an important result of this study as it is demonstrated that the application of the Sc.F. yields a notable increase in both the height and volume of the deformation. In the first set of experiments (E1) with AA1100 sheets, an increase of height up to 32% and deformation volume up to 47% was observed. The deformation of the AA6061 blank was less than the AA1100, however, falling less than 26% and 22% for the additional height of the dome shape and increase of the deformation volume respectively. Although the additional deformation from the application of the Sc.F. is dependent on the blank material, no consistent trend is observed in the deformation of the sheet metal by increasing the weight percentage of the Sc.F.

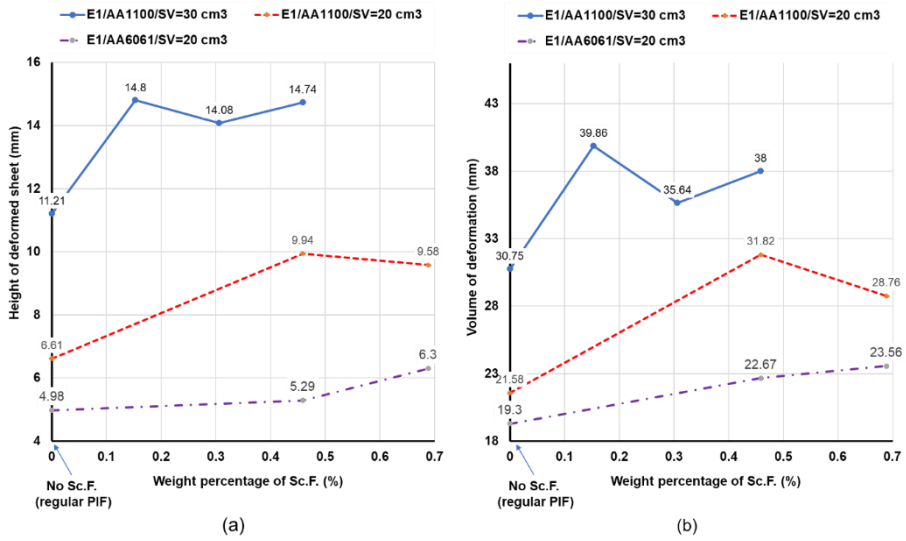

Fig. 5. (a) Height and (b) volume of the deformation

Shrinkage is usually a prominent challenge in the injection molding process. To quantify shrinkage in this study, diameter of the injected parts was measured one day after the experiment. The results of this measurement, as reported in **Error! Reference source not found.**(a), clearly demonstrate that using the Sc.F. technology resulted in a larger part due to less shrinkage of samples. However, no consistent trend was observed upon increasing the weight percentage of Sc.F. Shrinkage is more critical in the PIF process as the springback phenomena in sheet metal deformation would act in the reverse direction, which can result in delamination or a gap between the injected part and deformed metal. In order to investigate this phenomenon, a layer of adhesive coating was added on the surface of several blanks. These blanks were later processed in the same condition as main experiments. After one day, the hybrid samples were cut from the center. Investigating the cut section of these sheet metal-polymer samples provided further proof that the polymer melt with dissolved Sc.F. completely filled the deformed

area and there was no gap or delamination observed between the sheet metal and the polymeric part (see **Error! Reference source not found.**(b)). The layer of adhesive has been applied to make bonding between the injected part and the deformed sheet metal and keep them together to investigate the opposing effect of shrinkage vs. spring-back. Hence, the effects of this adhesive layer on the other aspects of the process were out of the scope of this work.

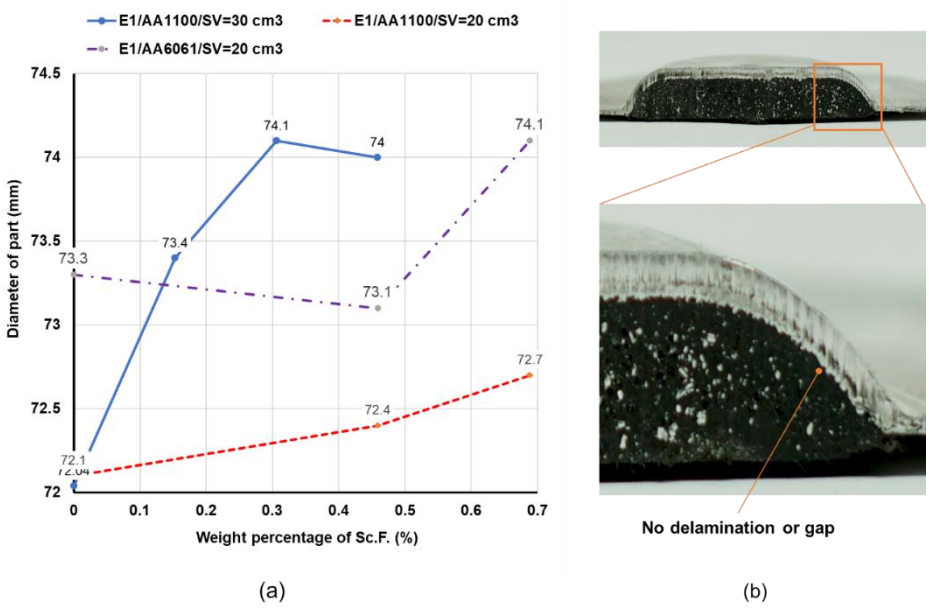

Fig. 6. (a) Diameter of the injected samples. (b) Cut section view of a hybrid sample produced by SCPIF

4.3 Weight and weight reduction

In previous studies, it was determined that the weight of the injected part in the PIF process is not only dependent on the shot volume but also on the formability of the sheet metal blank owing to the coupled filling/forming condition during the injection phase [12]. Hence, it is important to investigate the weight of the injected part to determine the consistency of the experiments and light-weighting capability of the SFPIF process. As seen in **Error! Reference source not found.**(a), the injected samples with Sc.F. assisted technology exhibit a higher weight for an identical shot volume. This phenomenon occurs as the use of Sc.F. increase the sheet metal deformation (see additional deformation in **Error! Reference source not found.**) and thus expanding the region in which the melt can flow into the cavity. In other words, the lessening of resistance enhances the flow of polymer melt into the cavity and reduces that which would otherwise escape through the gap between the barrel and the fights to the other side of the injection screw.

It was observed that although the weight of the injected part showed an increase upon the introduction of Sc.F., the total density of the hybrid part showed a reduction of up to 16 %. Moreover, this result shows that light-weighting increased with increase in weight percentage of Sc.F. until an optimum point, but then showed a decline. This result can be further explained by correlating the results of deformation (see **Error! Reference source not found.**(b)) and the weight of injected parts (**Error! Reference source not found.**(a)). This correlation indicates a decrease in deformation volume and an increase in sample weights, which in turn reduces light-weighting after the inflection point.

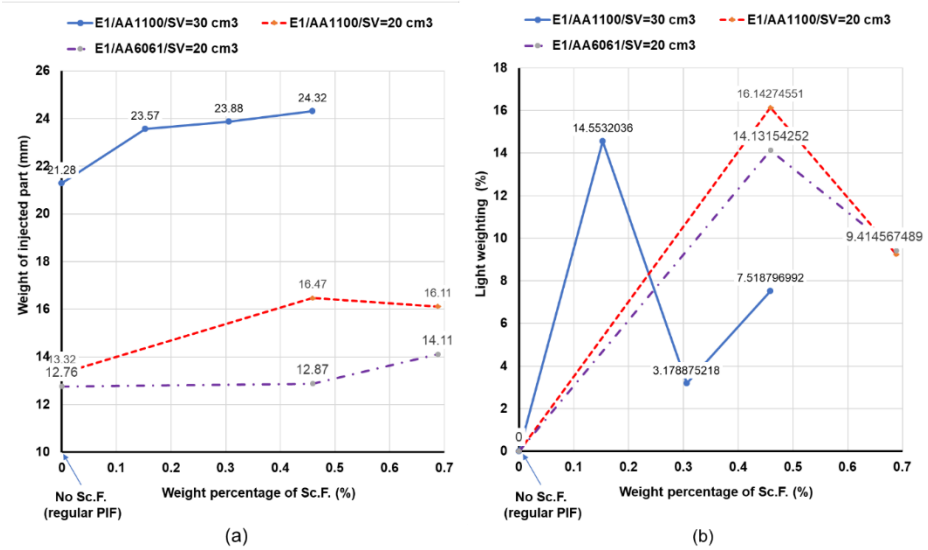

Fig. 7. (a) Weight of injected parts and (b) Light-weighting achieved with SCPIF

4.4 Micro-structure: Cell size and density

As the aim of the first set of experiments (E1) was to broadly understand the effects of integrating PIF and Sc.F. technology, the experiments were designed to elucidate changes in foam morphology with variances in both Sc.F. wt % and shot volume upon two aluminum alloys. A map of the cell densities vs cell sizes from E1 experiments plotted in **Error! Reference source not found.** shows the holistic effect of process and material variables on that foam morphology.

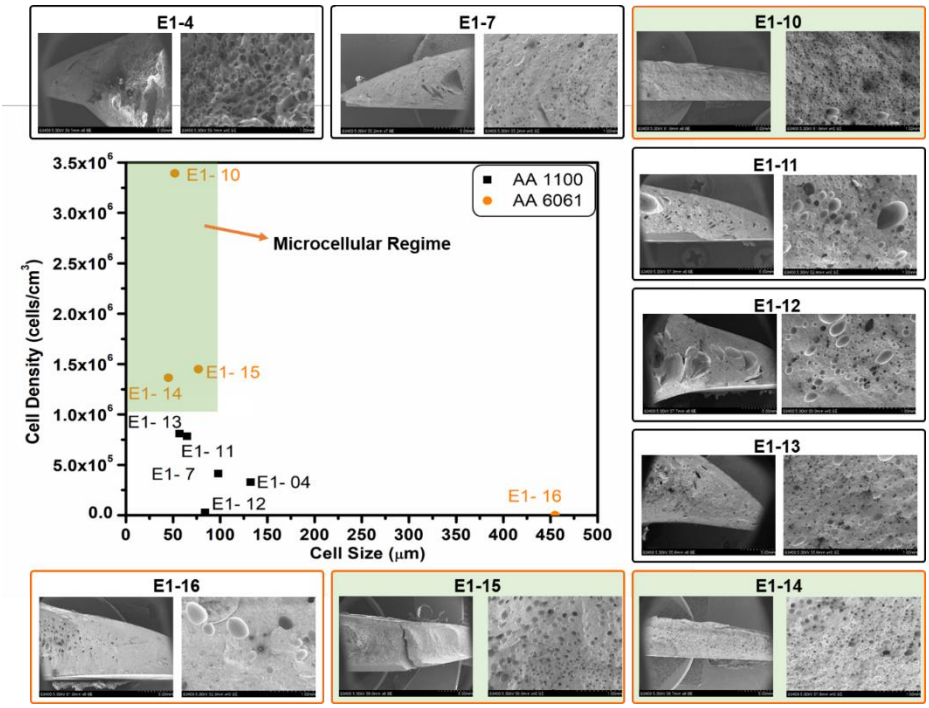

Fig. 8. Compilation of foam morphologies obtained in E1

Out of the 9 samples selected for SEM imaging, three samples exhibited a microcellular foam morphology (i.e. average cell diameters < 100 μm and cell densities > 1 x 10^6 cells/cm^3). These samples were produced in experiments (E1–10, 14 & 15) in which the AA6061 alloy was used as the sheet metal blank. But, all the samples were produced using the AA1100 sheets (E1– 4, 7, 11, 12, 13 & 16) showed inferior cell morphology (large cells with poor density) and blowholes underscoring the challenges associated with the integration concept of PIF and Sc.F. processes.

Two major reasons are hypothesized as to why the samples foamed in experiments with AA6061 sheet metal exhibited a consistently superior cellular morphology:

1. The use of the stiffer AA6061 sheet metal creates a higher pressure within the cavity and consequently a higher pressure drop at the end of the injection from suction induced by the plasticizing phase and/or the solidification of the gate. As a result, the foaming stage as the supercritical fluid in the polymer melt falls below the critical pressure resulting in either a diffusion into nucleated cells or nucleation of new cells [13].
2. The coupled filling/forming phase of the PIF process exhibits a similar set of conditions as the counter pressure method, caused by the resistance of the blank against the melt flow. This condition prevents the Sc.F. from escaping from the melt flow front and keeps the melt in a pressure higher than the supercritical until the end of the injection [14]. Clearly, it is now known that this condition will improve with the

use of AA6061 given its far greater yield stress over AA1100 which results in the application of the higher pressure inside the cavity from the beginning of the filling/forming phase.

As it was not possible to achieve the microcellular structure in the experiments conducted with AA1100 sheets, the second set of experiments was designed and performed to understand the effect of injection speed in different processing scenarios: (i) with 5 s packing pressure, (ii) no packing phase, and (iii) no packing plus decompression before plasticizing phase. A map of the cell density vs. cell size for E2 experiments is shown in **Error! Reference source not found.**.

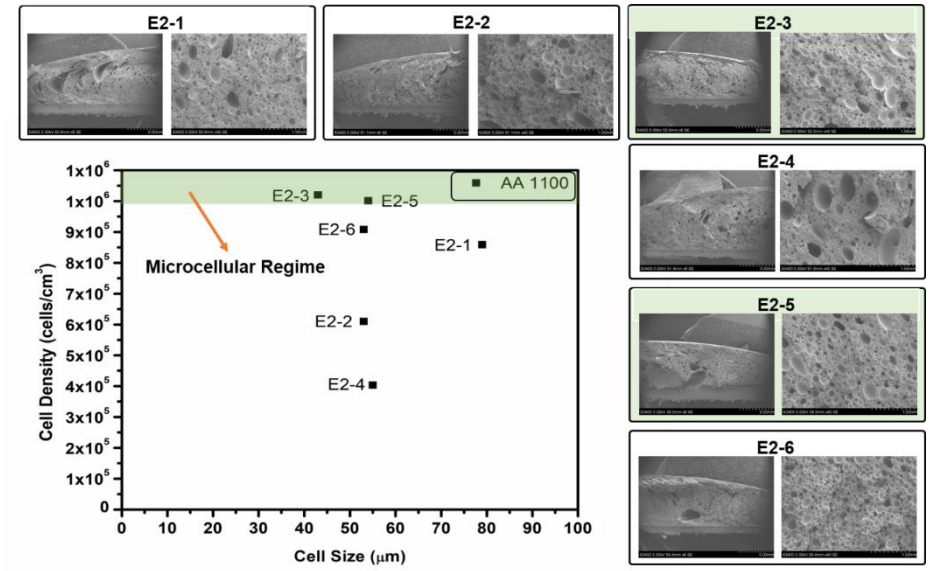

Fig. 9. Compilation of foam morphologies obtained in E2

It is clearly evident from **Error! Reference source not found.** that samples produced with no packing and/or decompression performed significantly better than the samples subjected to packing pressure vis-a-viz their smaller cell sizes and larger cell densities. Additionally, these experiments proofed that it is possible to achieve truly microcellular morphology with low strength sheet metals only by adjusting the process sequences and parameters. Such behavior is attributable to the acceptable performance of the second set of the experiments to control the pressure drop rate assuming the amount of the pressure drop would be the same as the first set. Other studies undertaken in microcellular injection molding also reported the importance of the drop rate, especially under low-pressure drop conditions [9].

5 Summary

The integration concept of PIF process with Sc.F. technology was successfully realized using the first set of the experiments. In the second set of the experiments, three processing scenarios were proposed to improve the cell nucleation and control the foaming process in SFPIF process. The effect of blank material and shot volume as design variables were investigated over a range of Sc.F. weight percentage. The following findings were derived from this study.

- Additional deformation due to the application of the Sc.F. was observed. Despite the dependency of deformation on blank material, no consistent trend was detected in the deformation of sheet metal to increase in weight percentage of Sc.F.
- Investigating the diameter of injected parts and cut section of hybrid samples further proved that this integration concept could completely eliminate the shrinkage issue, as no gap or delamination was observed on the hybrid parts due to the opposite reaction of shrinkage and springback.
- Despite the increase in the weight of the injected parts, density results demonstrated a good capability of this integration for lightweighting as up to 16 % weight reduction was achieved.
- The microstructure of Sc.F. foamed samples investigated by SEM showed that truly microcellular cell morphology was obtained as a result of conditions similar to counter pressure process created by use of the stiffer AA6061 sheet metal and/or higher pressure drop rates exhibited by eliminating the packing phase and setting decompression action before plasticizing.

Given the results of this feasibility study on the integration of PIF process with Sc.F. technology, future work should focus on improving this integration by further process optimization and introduction of more effective manufacturing procedures in order to control the nucleation process and attain the more-uniform microcellular morphology.

6 Acknowledgment

The authors would like to recognize the financial support by Robert Patrick Jenkins Professorship, and Dean’s Faculty Fellow Professorship. The authors would also like to acknowledge HASCO America Inc. for providing the metric mold base and standard mold components and Mr. Vinayak Khade for his help in the measurement of the samples. Saeed Farahani would like to acknowledge the financial support provided by Firestone Fellowship Award in Advanced Materials and Sonoco Fellowship in Automotive Engineering.

References

1. G. Kopp and E. Beeh, “New multi-material design concepts and high integration light metal applications for lightweight body structures,” in *Materials Science Forum*, 2010, vol. 638–642, pp. 437–442.
2. M. Grujicic *et al.*, “The potential of a clinch-lock polymer metal hybrid technology for use in load-bearing automotive components,” *J. Mater. Eng. Perform.*, vol. 18, no. 7, pp. 893–902, Oct. 2009.
3. M. M. Hussain, B. Rauscher, M. Trompeter, and A. E. Tekkaya, “Potential of Melted Polymer as Pressure Medium in Sheet Metal Forming,” *Key Eng. Mater.*, vol. 410–411, pp. 493–501, 2009.
4. C. Brecher *et al.*, “Integrative Production Technology for High-wage Countries,” in *Integrative Production Technology for High-Wage Countries*, Springer Berlin Heidelberg, 2012, pp. 17–76.
5. S. Farahani, A. F. Arezoodar, B. M. Dariani, and S. Pilla, “An Analytical Model for Nonhydrostatic Sheet Metal Bulging Process by Means of Polymer Melt Pressure,” *J. Manuf. Sci. Eng.*, vol. 140, no. 9, p. 091010, 2018.
6. W. Michaeli and R. Maesing, “Injection moulding and metal forming in one process step,” *Prog. Rubber, Plast. Recycl. Technol.*, vol. 26, no. 4, pp. 155–166, 2010.
7. S. Kazarian, “Polymer Processing with Supercritical Fluids,” 2000.
8. S. Aditya Pradeep, “An Investigation of Bimodal Cellular Distributions via Supercritical Fluid Assisted (SCF) Foam Injection Molding,” 2016.
9. J. Xu, *Microcellular injection molding*. 2011.
10. A. E. Tekkaya, M. M. Hussain, and J. Witulski, “The non-hydrostatic response of polymer melts as a pressure medium in sheet metal forming,” *Prod. Eng.*, vol. 6, no. 4–5, pp. 385–394, 2012.
11. S. Pilla, A. Kramschuster, L. Yang, J. Lee, S. Gong, and L. S. Turng, “Microcellular injection-molding of polylactide with chain-extender,” *Mater. Sci. Eng. C*, vol. 29, no. 4, pp. 1258–1265, May 2009.
12. S. Farahani, T. Zheng, and S. Pilla, “Hybrid Process of Forming-Injection Molding – Investigation of Polymer Melt Behaviour and Final Injected Part,” in *SPE-ANTEC*, 2019.
13. Q. Guo, J. Wang, C. B. Park, and M. Ohshima, “A microcellular foaming simulation system with a high pressure-drop rate,” *Ind. Eng. Chem. Res.*, vol. 45, no. 18, pp. 6153–6161, Aug. 2006.
14. S. C. Chen, P. S. Hsu, and S. S. Hwang, “The effects of gas counter pressure and mold temperature variation on the surface quality and morphology of the microcellular polystyrene foams,” *J. Appl. Polym. Sci.*, vol. 127, no. 6, pp. 4769–4776, Mar. 2013.